Russian Physics Journal, Vol. 51, No. 5, 2008

DEFORMATIONAL METHODS OF MATERIAL NANOSTRUCTURING: PREMISES, HISTORY, STATE OF THE ART, AND PROSPECTS

R. R. Mulyukov, A. A. Nazarov, and R. M. Imaev UDC 539.4.015: 548.4: 620.186: 621.77-79

Brief history of origin and development of methods of deformational nanostructuring of materials (DNM) also referred to as methods of severe plastic deformation (SPD) are presented. Principles and efficiencies of the most widespread DNM methods – torsion under quasi-hydrostatic pressure (THP), equal channel angular pressing (ECAP), and hydrostatic isothermal forging (HIF) – are analyzed. Results of pioneer research of the structure and properties of nanomaterials produced by these methods are given. Prospects for the DNM application in industrial technologies of metal treatment and product manufacturing are indicated.

INTRODUCTION

Over the last two decades, alongside with other nanomaterials, of great scientific and practical interest are bulk nanostructured materials – polycrystals with average grain sizes of the order of and less than 100 nm [1–6]. The production of these materials by compaction of metal nanopowders and the study of their properties were first reported by Soviet researchers (for example, see [7]). However, the boom of investigations in this area began in the late 80s – early 90s of the last century after H. Gleiter's publications who produced nanocrystals by the method of condensation in an inert gas with subsequent compaction [1]. Nowadays, there are about ten basic methods of producing nanomaterials [2–4]. Right after Gleiter's publications, a new approach to the production of nanostructured materials based on fragmentation of polycrystal grains under severe plastic deformation (SPD) was developed at the Institute of Problems of Metal Superplasticity of the Russian Academy of Sciences (IPMS RAS). The work in this direction was headed by R. Z. Valiev, R. R. Mulyukov, and G. A. Salishchev. The chosen direction of research, as was established subsequently, appeared successful and gave rise to methods of deformational nanostructuring of materials[1] (DNM) most widely used nowadays. These methods also referred to as the SPD methods include the methods of quasi-hydrostatic pressure (HPT), equal channel angular pressing (ECAP), and hydrostatic isothermal forging (HIF) [6]. A wide variety of nanostructured metals and alloys was produced by these methods, and pioneer investigations into their structure and properties were performed; due to this, the DNM is now a conventional method of producing nanomaterials widespread all over the world [6, 8, 9].

In the present paper, a brief review of premises and history of the DNM development is done, results of investigations into the structure and properties of nanostructured materials carried out at the IPMS RAS are presented, and a comparative analysis of scientific principles and technological efficiency of different DNM methods and prospects for their industrial applications are indicated.

[1]Despite the prevailing term severe plastic deformation [4], we prefer to use a more common term deformational nanostructuring. The use of this term is substantiated below.

Institute of Problems of Metal Superplasticity of the Russian Academy of Sciences, Ufa, Russia, e-mail: radik@anrb.ru. Translated from Izvestiya Vysshikh Uchebnykh Zavedenii, Fizika, No. 5, pp. 47–59, May, 2008. Original article submitted February 20, 2008.

1. PREMISES AND SCIENTIFIC PRINCIPLES OF METHODS OF DEFORMATIONAL NANOSTRUCTURING OF MATERIALS

1.1. Premises for the DNM methods

The fundamental principle of DNM is the well-known phenomenon of dislocation accumulation under plastic deformation of materials and formation of a dislocation substructure with misorientation boundaries [10]. This process occurs both under low- and high-temperature deformation, but its course and consequences differ radically for these two extreme cases.

Laws of evolution of metal microstructure under severe low-temperature plastic deformations were first studied by Soviet researchers V. I. Trefilov, Yu. V. Mil'man, and S. A. Firstov [11] and then systematized by V. V. Rybin [12]. These works demonstrated that irrespective of the initial structure, type of the crystal lattice of the material, and method of its deformation, the fragmented structure comprising intergranular high-angle boundaries is formed for high strain degrees. V. V. Rybin *et al*. [12] suggested an ordered qualitative and quantitative theory of crystal fragmentation. According to its concepts, mesodefects are formed on the grain boundaries and joints under severe plastic deformation, and relaxation of their long-range stresses causes the formation and evolution of new misorientation boundaries whose misorientation angles increase up to a few tens of degrees. However, there were two main problems hindering the production of nanostructures by the conventional methods of metal treatment under pressure: first, monotonic deformation yielded elongated fragments and second, after accumulation of a certain critical fragmented structure, being still far from the equiaxial nanostructure, the material failed [12]. In this regard, special deformation schemes were required to reach very high degrees of strain without fracture of the material.

The laws of evolution of the material structure under hot plastic deformation were studied at the IPMS RAS in connection with the necessity of producing an ultrafine-grained superplastic structure [13]. The basic mechanism of reducing the grain sizes under hot deformation is dynamic recrystallization. In this process, the size of recrystallized grains d of the material depended on the deformation rate and temperature: $d = f(\dot{\varepsilon}, T)$ [14]. The size of dynamically recrystallized grains can be reduced by decreasing the temperature or increasing the deformation rate. In principle, it would be possible to produce grain sizes of about d = 100 nm and smaller by material deformation at the appropriate (low enough) temperature. However, this cannot be made in practice for the following reasons. First, the critical deformation necessary to initiate the dynamic recrystallization increases significantly with decreasing temperature. Because of this, high strain degrees are required to produce a completely recrystallized nanostructure. At the same time, the technological plasticity of coarse-grained materials is low at a relatively low temperature; therefore, it is impossible to produce completely recrystallized microstructure at this temperature. Second, in the case of deformation at low temperatures, the deformation is localized, and the grain sizes are reduced only in local regions of the material. Hence, it was also necessary to develop special schemes and modes of nanostructuring by hot deformation.

It turned out that the fundamental and technical problems related with the possibility of application of superhigh degrees of plastic strain to the material without its fracture and with uniform reduction of grain sizes could be solved, which was made practically simultaneously for both deformation modes and gave rise to three of the most investigated and widespread DNM methods, namely, HPT, ECAP and HIF methods.

1.2. Principles of the HPT method

In the middle 1980s, V. I. Levite *et al*. [15] first demonstrated the principal possibility of nanostructuring of metals and alloys under plastic deformation exactly by the method of torsion under quasi-hydrostatic pressure. Levite *et al*. [15], using the method of torsion under high pressure, nanostructured nickel specimens with thickness of a few fractions of a millimeter at room temperature. Due to the constrained deformation conditions (high hydrostatic pressure), they succeeded in deposition of a significant deformation energy into the material without material fracture.

The HPT method of material nanostructuring under deformation is the simplest method of producing a nanostructure with grain sizes reduced to d = 10–20 nm [5, 17, 18] and even completely amorphous alloys (for example, TiNi) [4]. This remarkable express method is most often used to produce nanostructured specimens to study

their physical properties. Many pioneer results demonstrating the extraordinary properties of bulk nanomaterials were obtained for specimens of this type. In the HPT method, the specimen shaped as a disk with a thickness of a few fractions of a millimeter is placed between the block heads and compressed under a pressure of several GPa. The rotating upper head forces the specimen to shear under the action of the surface friction force. Rotation of the mobile head through different angles yields different strain degrees. For pure shift, the degree of strain γ for points of the specimen located along the circle of radius r can be calculated from the formula $\gamma = 2\pi rN / L$, where N is the number of revolutions of the mobile head and L is the specimen thickness [4]. From this formula it follows that the degree of strain linearly increases from zero in the center of the specimen to a maximum value at the specimen edge. Meanwhile, as demonstrated by numerous investigations, the structure is sufficiently uniform throughout the entire specimen volume for sufficiently great number of head revolutions, which is apparently caused by a high hydrostatic pressure produced in the examined deformation scheme. This provides high uniformity of stress and strain distributions [4]. Thus, there is certain arbitrariness in the definition of the γ value.

Numerous investigations into the structure evolution of various metals and alloys subjected to HPT to different strain degrees demonstrated that the nanostructured state is formed in this process [17, 18]. In this case, three subsequent stages were identified for specific strain degrees, and a specific structure corresponded to each stage. First, the cellular structure is formed upon deformation in which dislocation tangles and pileups fill the entire cell volumes. In the second stage, a mixed cellular/granular structure arises. In the third stage, a uniform granular nanostructure is formed without dislocations inside grains and with nonequilibrium grain boundaries (GB), that is, the structure with increased density of grain-boundary dislocations. The stage character is independent of the homological deformation temperatures (for pure metals), energy of packing faults (EPF) (in solid solutions), and phase composition (for multiphase alloys); however, the enumerated factors influence the strain degrees for which these stages are observed and the structural characteristics in the steady stage. Thus, some researches pointed out that the minimum grain sizes obtained by the HPT method decrease with the EPF [19] and homological HPT temperature [20].

The structure evolution for torsion under high pressure at room temperature is similar to that observed for materials deformed at increased temperatures, for example, by compression when the process of dynamic recrystallization proceeds. Some distinctions are caused by different internal stressed achieved in the examined processes. Due to an extremely high level of these stresses, the self-organization of the structure subjected to torsion under pressure is universal in character and is essentially independent of the bond type, initial microstructure, phase composition of the material, size and distribution of phase particles, degree of alloying of the solid solution, characteristics of deformation carriers, and other factors. As is well known, the dynamic recrystallization at increased temperatures proceeds under relatively low stresses and depends significantly on the above-enumerated and many other factors. However, after nanostructuring, the materials in the steady stage of torsion under high pressure behave similarly to the fine-grained materials under conditions of superplastic flow. That is, as under conditions of superplastic flow, the GB behavior for torsion under high pressure becomes universal and independent of the material type. However, this is observed after accumulation of a certain threshold defect density under SPD. For this reason, it is pertinent to refer the DNM method based on the HPT scheme to the class of the SPD methods.

1.3. Equal channel angular pressing

The ECAP method of repeated plastic deformation of specimens was developed by V. M. Segal and V. I. Kopylov *et al*. [21]. It consists in specimen pressing through two crossed channels of equal diameters. The specimen is deformed in the region adjacent to the plane of channel crossing, and the deformation is close in character to a simple singular shear along this plane [22]. The deformation degree corresponding to this shear is $\varepsilon = 1.15$ when the angle between the channels is equal to 90° [22]. Repeated passages of the specimen through the channels allow the desirable degree of strain and hence of structural changes to be obtained; in this case, the specimen shape will be retained except regions near its ends. The ECAP method was originally created as a method of metal treatment under pressure that allowed metals to be subjected to high degrees of plastic strain mainly by its simple shearing without considerable change of the specimen geometry. The ECAP method was one of the candidates to the DNM method, and

in [23] it was first demonstrated, taking copper as en example, that metals with grain sizes of several hundreds of nanometers can be produced by this method.

An advantage of the ECAP method is that overall dimensions of specimens produced by this method can be much greater than those produced by the HPT method. Parallelepiped specimens with cross sectional sizes up to 20 mm are typically used. A combination of the ECAP method with the conform-process can be perspective for manufacture of long nanostructured semifinished items [24]. However, an essential disadvantage of the ECAP method is the restriction on the cross sectional sizes of these semifinished items. Requirements imposed on the strength of the equipment material, quality of greasing, and power of press equipment increase sharply with cross sectional area of specimens.

Despite a large number of microstructural studies, laws of reduction of grain sizes during ECAP have not yet been understood completely. However, the common features of this process that allow conclusions about its efficiency to be drawn can be considered established.

Numerous studies of the evolution of metal substructure under monotonic deformation by the conventional methods (shearing, rolling, etc.) demonstrate that the basic mechanism of grain size reduction is the formation of microstrips misoriented relative to the initial grain and lying in planes close to the plane of the maximum shear stress [12, 25]. The ECAP is the deformation process with changeable deformation route, which allows this process to be varied. The deformation route is changed by rotation of the specimen between two successive passages. After the first passage of the specimen through the equipment, a system of microstrips parallel to the channel crossing plane (the shear plane) [26] is formed. Subsequent passages with specimen rotation around the axis through 90° (according to the standard classification, by routes B_A and B_C) lead to the formation of the microstrip boundaries lying in other planes which, being crossed with initial ones, result in the formation of closed fragments close to equiaxial ones. For this reason, routes B_A and B_C result in the fastest formation of equiaxial nanostructures [27]. However, it is well known that each substructure is a response of the material to concrete monotonic loading; change of the deformation route promotes fracture of the old substructure and creation of a new one characteristic of the new conditions [12]. Hence, the routes with rotations lead to a partial fracture of previously formed boundaries, and misorientations are accumulated more slowly than under monotonic deformation. Therefore, routes B_A and B_C of the ECAP result in the formation of the equiaxial nanostructure with mainly low-angle boundaries [28]. Most clearly this law is manifested if we compare two extreme cases of routes *A* when the specimen is not rotated and *C* when it is rotated through 180°. In the first case, the structure develops continuously, and elongated grains are formed with large-angle misorientations between them. In the second case, the equiaxial substructure is formed with low-angle misorientations [28].

On the other hand, for deformation along route *A*, evolution of one and the same system of microstrips occurs, and the nanostructure formed after multiple passages consists of grains elongated in the direction close to the specimen axis.

In connection with the aforesaid and because of a large amount of energy spent on friction between the specimen and equipment, the ECAP method is rather energy consuming process of deformational nanostructuring that uses incompletely the DNM potential.

The efficiency of reduction of grain sizes under monotonic deformation, including application of route *A* of the ECAP, can be increased by increasing the mobility of grain boundaries that facilitates local migration of longitudinal GB and formation of transverse GB and equiaxial structures [29]. Processes of recovery and recrystallization are important for transformation of deformation substructures into equiaxial low-energy granular structure stable under subsequent deformation. Investigations demonstrated that the dynamic recrystallization occurs in the ECAP process in metals with low melting temperature (Al and Cu) already at room temperature, and in metals with high melting temperature at moderately high temperatures [30]. This means that depending on the deformation temperature, the nanostructure can be formed by the ECAP method by one of the two basic mechanisms, namely, by formation of the deformation boundaries due to crossing of microstrips at low temperatures and due to recrystallization at high temperatures. It seems likely that exactly these mechanisms determine the class to which the ECAP process can be referred, namely, severe plastic deformation at low temperatures and softer deformation treatment with partial dynamic recrystallization at relatively high temperatures.

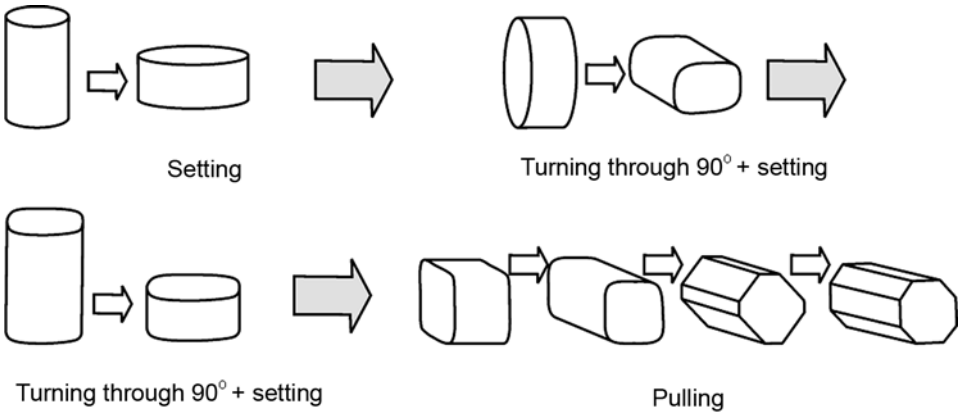

Fig. 1. Scnematic of hydrostatic isothermal forging.

1.4. Hydrostatic isothermal forging

The problem of complete use of the dynamic recrystallization potential to reduce grain sizes to produce the nanostructured state had been solved by the HIF method [31–35]. To this end, the fulfillment of three basic requirements was provided in one process, including a significant decrease of the isothermal deformation temperature, retention of the technological plasticity of the material, and uniform evolution of the dynamic recrystallization process.

To elaborate the technological route of producing the nanostructured state for this or that material by deformation, the specimen is first studied using modeling. To this end, cylindrical specimens deformed by compression with different rates and at different temperatures are used. Based on these investigations, a dependence of the recrystallized grain size d on the temperature T and deformation rate $\dot{\varepsilon}$ is drawn, from which the temperature and rate conditions of producing a uniform fine-grained microstructure of the material are determined. The main point here is to produce a uniform microstructure, at least, in the central part of the specimen. As a rule, a highly uniform microstructure is produced by deformation under the superplastic temperature and rate conditions, when the grain sizes do not exceed d = 10–15 μm [13], that is, at relatively high temperatures and low deformation rates. The dependence $d(T,\dot{\varepsilon})$ also yields information on the temperature and rate conditions at which nanodimensional grains are formed. They are relatively low temperatures or high deformation rates. However, a nonuniform partly recrystallized microstructure is formed in the central part of the specimen under such deformation conditions.

Figure 1 shows the schematic of hydrostatic isothermal forging developed and used to produce nanostructured (NS) semifinished items of different materials. A specimen is forged with the rate and at the temperature that had been chosen during preliminary investigations. The schematic of hydrostatic isothermal forging facilitates uniform deformation distribution over the specimen volume. However, the uniformity of recrystallization processes and hence of the microstructure is provided not only by the proper forging temperature and rate but also by its schematic. The specimen is subjected to hydrostatic forging until 100% rectrystallization of its volume is achieved. The grain size is determined by the Zener–Hollomon formula [14]. Several points should be mentioned here. As can be seen from Fig. 1, the specimen is subjected to hydrostatic isothermal forging to avoid significant contact friction, that is, with relatively slow deformation degree during each transition. After forging, the specimen shape is close to the initial one.

The technological plasticity of metals and alloys increases due to reduced microstructure grain sizes. Further deformation under the same temperature and rate conditions causes the superplastic flow of the material; this is often the case for metals and alloys [13]. A decrease in the temperature of subsequent deformation (given that the deformation rate remains unchanged) provides further reduction of microstructure grain sizes. Repeated HIF at the decreased temperature allows a completely recrystallized uniform microstructure to be produced already with much less recrystallized grain sizes. Additional reduction of microstructure grain sizes results in the increased technological

plasticity of the material (the superplastic flow), which allows the hydrostatic forging temperature to be decreased again. Thus, HIF with stage-by-stage decrease in temperature enables the grain sizes in the material to be reduced to nanosizes without material fracture. The final deformation temperature is chosen from the $d(T, \dot{\varepsilon})$ dependence.

Some important points should be mentioned. The number of stages, the temperature difference between the successive stages ΔT_i and between the first and last stages ΔT, and the number of transitions at different stages depend on the material type and initial microstructure. The key point here is producing a uniform recrystallized microstructure at each stage. The non-recrystallized volumes of the material that remain after treatment at increased temperatures are inherited by the subsequent treatment at lower temperatures, since the deformation is localized mainly in the fine-grained fraction. This finally leads to a bimodal microstructure. The deformation rate at the first and subsequent stages is chosen so that to reduce the influence of deformation heating and hence to provide uniform recrystallization processes. In the case of HIF with a hydraulic press, the deformation rate is typically $\dot{\varepsilon} = 10^{-3}$–$10^{-2}$ s^{-1}. At each stage of reducing the microstructure grain sizes, the material is transformed into the superplastic state, thereby facilitating the formation of a uniform nanostructure.

The HIF method is universal; it can be used not only for relatively technological (plastic) metals and alloys but also for almost undeformable materials. For identical consumed energies, the HIF method allows a greater amount of energy to be deposited into unit mass than the ECAP method, since in the first case, the energy spent to overcome the friction and counterpressure forces is much less than in the second case. As a result, the HIF method can be used to produce more bulky nanostructured semifinished items and nanostructured billets than the ECAP method with the existing presses and simple commercial equipment. Therefore, the HIF method is the technologically most attractive DNM method. Bulky nanostructured billets of several tens of industrial alloys based on titanium, nickel, aluminum, magnesium, and steels were produced by the HIF method [6].

2. MULTILEVEL STRUCTURE OF NANOSTRUCTURED METALS

Since grain boundaries occupy a significant fraction of the nanostructured material volume, they play the determining role in the properties of these materials. Therefore, studies of the nanomaterial structure are mainly directed on elucidation of the GB structural features. In the study of the GB structure in nanomaterials produced by the DNM, various methods were used to establish the GB special features on microstructural, atomic, electronic, and superfine magnetic levels, including x-ray analysis, EXAFS spectroscopy, transmission electron microscopy (including high-resolution one), Mössbauer spectroscopy, field ion and electron microscopy, and field electron spectroscopy.

The main feature of the GB structure confirmed by numerous researches is the following.

On the one hand, the grain boundaries in freshly prepared nanomaterials are in a specific nonequilibrium state in which they contain dislocations incorporated during deformation treatment and have increased energy and long-range stress fields. This can be seen from specific GB images recorded by the method of field electron microscopy and characterized by the absence of strip contrast typical of the grain boundaries in well annealed polycrystals and by the presence of extinctional contours near the grain boundaries [36, 37]. At the same time, the visible crystallographic GB width does not differ from the width of the equilibrium grain boundaries and makes $\delta_{cr} \approx 0.5$–1 nm, and the long-range distortions are elastic in character. Direct electron microscopic observations demonstrate that regions with significant, up to 1–3%, lattice distortions are observed in nanocrystals near the grain boundaries; the thickness of these regions is about 6–10 nm [38].

On the other hand, investigations by the methods of Mössbauer and field electron spectroscopy demonstrated that the physical GB width is much greater. Mössbauer spectroscopy was used to investigate nanostructured iron with grain sizes $d = 220$ nm produced by the HPT method and, for a comparison, the same material with grain sizes $d = 15$ μm [39]. An analysis of the Mössbauer spectra demonstrated that the superfine magnetic structure of nanostructured iron was complex in character, thereby indicating the presence of metal atoms in two clearly distinguished states. It seems likely that atoms inside grains were in the first state whose parameters were typical of the conventional crystal state. The second state had significantly different but fixed parameters that were reproduced for different specimens. A comparative analysis of the subspectra corresponding to this state at temperatures $T = 77$ and 300 K was used to determine its Debye temperature. It was by $\Delta T = (150 \pm 50)$ K lower than the corresponding

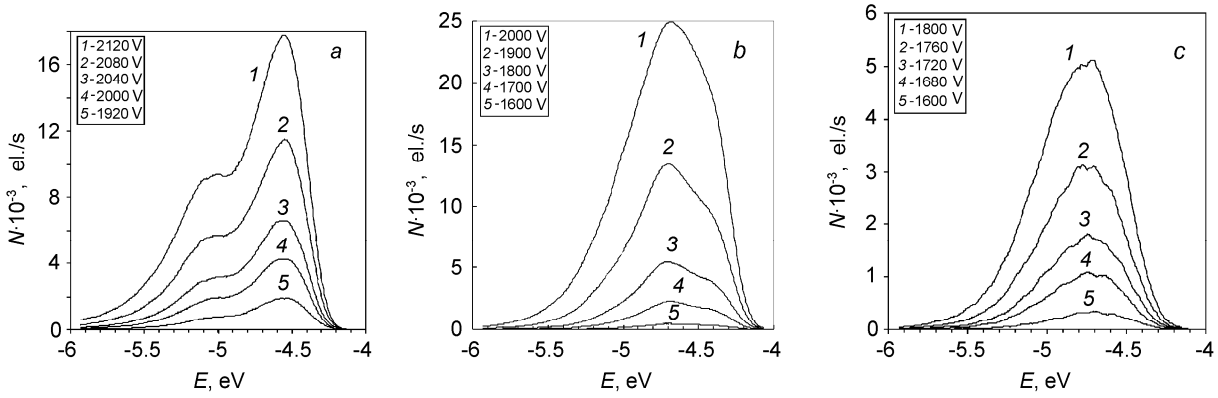

Fig. 2. Distributions of autoelectrons over total energies for the emission voltages indicated in the insets and measured for the surface fragments comprising a grain boundary (*a* and *b*) and removed far from the grain boundaries (*c*).

temperature for iron crystals. It is reasonable to assume that the grain boundary atoms are in the second state. Based on this assumption, comparing the relative intensities of the Mössbauer subspectra, it is possible to determine the width of the spatial region at the grain boundaries occupied by these atoms; it appeared equal to $\delta_{ph} \approx (11 \pm 1.5)$ nm.

Integrated studies of the atomic structure and electron properties of nanostructured nickel and tungsten were carried out in [40, 41] by the methods of field ion microscopy, field electron microscopy, and field electron spectroscopy. In these works, energy distributions of autoelectrons emitted from regions of nanomaterials belonging to grains and close to grain boundaries were investigated. It turnes out that an additional peak arises in the low-energy part of the total energy distribution of autoelectrons emitted from the vicinity of grain boundaries ~10 nm wide or bending of the leading edge of this distribution (Fig. 2*a* and *b*) are observed in comparison with the energy distribution of electrons emitted by the crystal (Fig. 2*c*). Hence, the electronic structure of the GB region in nanomaterials also differs significantly from the electronic structure of crystals. Numerical modeling of the total energy distribution of emitted electrons by the sum of distributions of two types corresponding to crystal and grain-boundary electrons demonstrated that the electron work function and the density of electricity carriers in the GB vicinity were smaller than their corresponding values inside the grain body [42]. Based on this, the assumption was made that the special features of the energy distribution of electrons emitted from the nanostructured metal can be explained by the current routs with reduced work functions that arose along the grain boundaries.

Thus, the physical GB width in nanomaterials estimated from the results of investigations of superfine and electronic structure considerably exceeds the crystallographic width $\delta_{cr} \approx 0.5$–1 nm estimated from the microstructural studies. In spite of the fact that at distances from the grain boundaries exceeding δ_{cr}, no significant distortions in the lattice structure were observed with a high-resolution electronic microscope, the dynamic state of atoms and the electronic structure can differ significantly due to high elastic stresses produced by the boundaries. Therefore, the notion was introduced of the specific *grain-boundary phase* with the thickness $\delta_{ph} \approx 10$ nm possessing the physical parameters that differed significantly from the corresponding parameters of the crystal or *granular phase*.

Thus, investigations of the nanostructured materials carried out on different structural levels demonstrate the presence of two main features in their structure: nonequilibrium GB state and biphase composition. Based on the foregoing, the following structural model of nanomaterials produced by the DNM method was suggested.

As indicated above, V. V. Rybin *et al*. [12] have demonstrated that mesodefects consisting of dislocations are formed at the grain boundaries and their joints under plastic deformation. Under severe plastic deformation, these mesodefects have extremely high densities. Their unshielded stress fields create high internal stresses resulting in increased GB energy and elastic distortions of the GB themselves and adjacent regions. As a consequence of these distortions, the lattice dynamics, electronic structure near the grain boundaries, diffusion coefficient, and some other properties change significantly in comparison with the conventional crystalline materials. The nanostructured material

TABLE 1. Mechanical Properties of the VT6 Alloy at Room Temperature

Material state	σ_u, MPa	$\sigma_{0.2}$, MPa	δ, %	ψ, %	σ_{-1}, MPa
Nanostructured (after HIF), d = 400 nm	1350	1300	8	60	690
Nanostructured (HIF + cold rolling)	1500	1460	8	55	–
Fine-grained (quenching + aging), d = 10 μm	1050	980	9	35	580

appears to be spatially subdivided into two phases referred to as granular and grain-boundary phases. The granular phase has properties characteristic of the single crystals; materials in the conventional coarse-grained state have virtually the same properties. The atoms of the grain-boundary phase are in a certain dynamically excited state and as a consequence, have the decreased Debye temperature and increased energy; the parameters of their superfine magnetic and electronic structure have fixed values that differ significantly from the parameters of the granular phase. The thickness of the grain-boundary phase Δd is by an order of magnitude greater than the crystallographic width of the boundaries; according to the available experimental data, it is about 10 nm.

The suggested structural model describes well the experimentally observed quantitative characteristics of nanomaterials, such as the root-mean-square elastic stresses, excess energy, and increase in volume [43, 44] as well as the electronic, elastic, and other physical properties [3, 5].

3. PROPERTIES OF BULK NANOMATERIALS

One of the main consequences of deformation nanostructuring of materials is a significant increase in the material strength; moreover, unlike the conventional methods of treatment by pressure resulting in a sharp reduction of plasticity, the DNM method retains the plasticity of the material on a satisfactory level.

As an example, Table 1 presents values of the mechanical characteristics of the VT6 nanostructured titanium alloy produced by the HIF method [45].

From Table 1 it follows that the VT6 nanostructured alloy has the ultimate strength σ_u and the fatigue limit σ_{-1} exceeding by 30 and 20%, respectively, the corresponding characteristics of the fine-grained alloy of the same composition hardened by quenching and aging. Additional cold rolling increases the ultimate strength of the nanostructured alloy by 10–12%, retaining its plasticity. Analogous results were obtained for other titanium alloys subjected to nanostructuring by the HIF method [31, 46].

The increase in the fatigue limit of the VT6 alloy caused by nanostructuring is observed for the entire interval of working temperatures for this material, up to T = 400°C. Further increase in temperature leads to the reverse effect, namely, to a sharp reduction of the flow stress and manifestation of the superplasticity effect. Moreover, the superplasticity effect in the VT6 nanostructured alloy is observed already at temperatures by 200–300°C less than the superplasticity temperature interval for the conventional fine-grained material [47].

The superplasticity at relatively low temperatures appeared universal and was also observed for almost undeformable alloys. In the Inconel 718 heat-resistant nickel alloy, the nanoduplex structure with grain/particle sizes d = 80 nm was produced by the HIF methods [48]. The nanomaterial also demonstrated superplastic behavior at relatively low temperatures: its lower temperature threshold of superplasticity was 650°C as compared with 800°C for the microcrystalline alloy of the same composition [48].

Figure 3 shows that nanostructuring down to grain sizes d = 100 nm changes radically the behavior of the Ti–25Al intermetallic alloy [49]. The material fragile by the nature demonstrates superplastic behavior in the nanostructured state at temperatures T = 600–1000°C, and at T = 600°C, elongation reaches δ = 780%. In this case, the material plasticity at room temperature should especially be noted: elongation unexpectedly increases from zero to δ = 4.8%.

To understand a nature of this effect, the absorption of the lattice dislocations by grain boundaries was studied in [49] for the Ti–25Al alloy with different grain sizes. Specimens with grain sizes d = 300 nm and 27 μm were deformed by compression at ε = 2% and then annealed for 15 min at different temperatures. After deformation, the incorporated lattice dislocations were observed virtually in all boundaries. After subsequent annealing at the

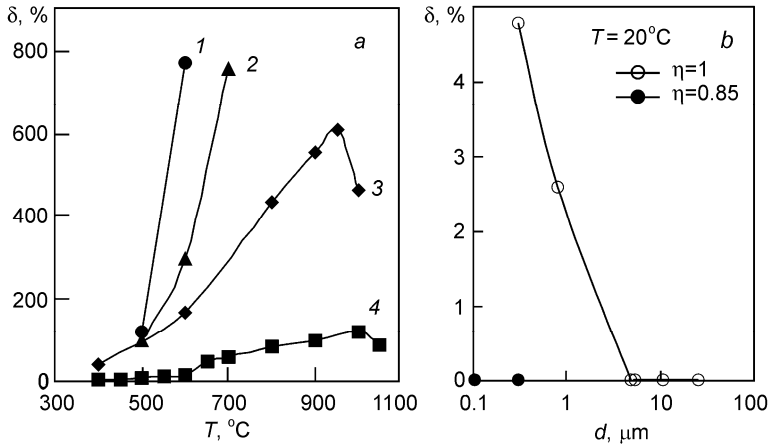

Fig. 3. Relative elongation δ of specimens made from the Ti–25Al alloy versus the grain size d ($\dot{\varepsilon} = 6.4 \cdot 10^{-4}$ s^{-1}): *a*) at increased temperatures for $d = 100$ (curve *1*), 300 (curve *2*), and 800 nm (curve *3*) and 8.5 μm (curve *4*); *b*) at room temperature; here η denotes the degree of the long-range order.

temperatures depending on the grain sizes, the contrast from these dislocations disappeared. The temperature dependence of the relative fraction of grain boundaries in which dislocations disappeared $v(T)$ was determined. Results of investigations demonstrated that the function $v(T)$ for the Ti–25Al nanostructured alloy was displaced to the left by ~400°C in comparison with the coarsely grained crystalline alloy, that is, dislocations disappear in the nanomaterial at much lower temperatures than in the conventional materials. The relaxation activity of the grain boundaries in the nanostructured intermetallic alloy was observed even at room temperature. It seems likely that the reduction of grain sizes to the nanostructural level in the Ti–25Al intermetallic alloy activates the grain-boundary diffusion even at room temperature. This demonstrates the possibility of development of the grain-boundary slipping mechanism in this material at room temperature. It seems likely that the plasticity arising at room temperature and the decrease in the superplasticity temperature to $T = 600$°C ($0.47T_{melt}$) testify to a significant contribution of this mechanism to the plastic deformation of the Ti–25Al nanostructured alloy.

Obviously, the result obtained can be generalized to the conventional metals and alloys. Reduction of grain sizes to the nanostructural level significantly decreases the temperature at which the grain-boundary slipping mechanism is activated in metals and alloys. This fact has two important consequences. First, the increase of plasticity with reduction of grain sizes makes nanostructuring by the HIF method feasible. Second, superplastic deformation at relatively low temperatures considerably facilitates superplastic pressing and molding of alloys.

A significant increase in the grain-boundary diffusion coefficient of nanomaterials is confirmed by direct measurements. For example, the diffusion coefficient of the ^{59}Fe isotope in nanostructured palladium at the temperature $T \approx 100$°C reached values characteristic of coarse-grained palladium at $T = 900$°C [50]. Such abnormal behavior was observed until the specimen annealing at the temperature $T = 230$°C and disappeared after annealing at the temperature $T = 260$°C. Annealing does not cause the grain sizes to increase significantly; however, it is accompanied by transition of grain boundaries into a more equilibrium state. Thus, the size effect (an increase in the GB volume fraction) plays an important role in the diffusion properties of nanocrystals as well as in their other properties together with the nonequilibrium GB structure which results in an increase of the grain-boundary diffusion coefficient by 1–2 orders of magnitude in comparison with the grain boundaries of coarse-grained polycrystals. Theoretical investigations and atomic modeling of the diffusion process demonstrate that in accordance with the experiments, the nonequilibrium GB state can actually cause an increase in the GB diffusion coefficient by 1–2 orders of magnitude [51, 52].

Nanostructuring by the DNM method results in significant changes of other physical properties of the materials, including their thermal, elastic, inelastic, electric, and magnetic properties. Thus, according to [53], the modules of elasticity of copper and nickel with average grain sizes $d \approx 100$ nm were by 10–15% less than those of

coarse-grained polycrystals. The internal friction of a nanostructured material had the level of its amplitude-independent component 3–5 times higher in comparison with coarse-grained specimens and comparatively weak amplitude dependence [54].

In the nanostructured ferromagnetic materials, changes of the saturation magnetization and temperatures of magnetic phase transitions were detected in [55, 56]. For pure metals, the coercive force monotonically increased with reduction of the grain sizes [57]. In magnetically hard materials, the coercive force and residual induction can also be increased by reduction of the grain sizes. However, this dependence is nonmonotonic in character, which is caused by change of the phase composition under deformation [58].

From the practical viewpoint, the established possibility of increasing the strength, plasticity, and mechanical workability of a magnetically hard material with simultaneous retention of its highly coercive state by reduction of the grain sizes is very important. This dependence is also nonmonotonic in character. For example, in Fe–Cr–Co alloys in the highly coercive state, the effect of a nonmonotonic increase in the plasticity is connected with partial dissolution of modulated $\alpha_1 + \alpha_2$ structures in slipping strips [59, 60].

A large volume fraction of grain boundaries and an excited state of atoms in them result in additional dispersion of conduction electron in nanomaterials, which is manifested through an increase in their electrical resistance. The formation of the nanostructured state of copper doubles its electrical resistance at the temperature of liquid nitrogen in comparison with coarse-grained copper [61]. Annealing of specimens causes restoration of the electrical resistance, and the sharpest decrease in the resistance, equal to ~20%, is observed at temperatures T = 150–200°C. Microstructural studies demonstrate that exactly in this temperature interval, the grain boundaries in nanostructured copper are transformed from the nonequilibrium into equilibrium state. This allows the special features of the behavior of electrical resistance to be related with the GB state [61].

The nanostructured metals possess the electron work function less than that of coarse crystalline metals; for example, according to [62], the difference is 0.8 eV for nanostructured tungsten.

4. PROSPECTS FOR APPLICATION

Thus, treatment by the DNM method results in a significant change of the physical and mechanical properties of materials that opens the possibilities for functional and constructional applications of nanomaterials. From the tendency of applied research in this direction, it can be concluded that these applications of nanomaterials can be developed in two directions.

The first direction is a direct manufacture of parts of machines and mechanisms from nanostructured semifinished items. These products will possess an increased strength and fatigue resistance and simultaneously improved functional properties. For example, manufacturing of medical equipment from nanostructured titanium is perspective [4]. The use of nanomaterials as damping materials will allow simultaneously their internal friction and strength to be increased and hence noise caused by vibration of machines and mechanisms to be suppressed considerably and thereby its harmful effect on the accuracy of measuring devices to be reduced. Nanostructuring will allow the hysteresis properties of magnetically hard materials to be improved, providing simultaneously high strength of highly coercive magnets and their mechanical workability. The established reduced work function of electrons in nanostructured metals can be used to develop highly efficient electron sources.

The second direction is superplastic treatment of nanostructured materials. A significant decrease in the temperature of superplastic deformation after nanostructuring makes superplasticity promising technology for practical applications. With the use of superplastic pressing, molding, and treatment technology combining molding with welding under pressure, it will be possible to expand significantly the assortment of products with irregular profiles required for manufacturing of aviation engines, power engineering, and other branches of industry [63]. Especially perspective is manufacturing of blades and disks for aviation engines of new generation using these technologies. The formation of a nanostructure results in better weldability of alloys under pressure with simultaneous improvement of the weld quality. Based on the scientific results obtained, the integrated technology combining welding by pressure with superplastic molding have been developed. One of the examples of application of such technologies is the model of the

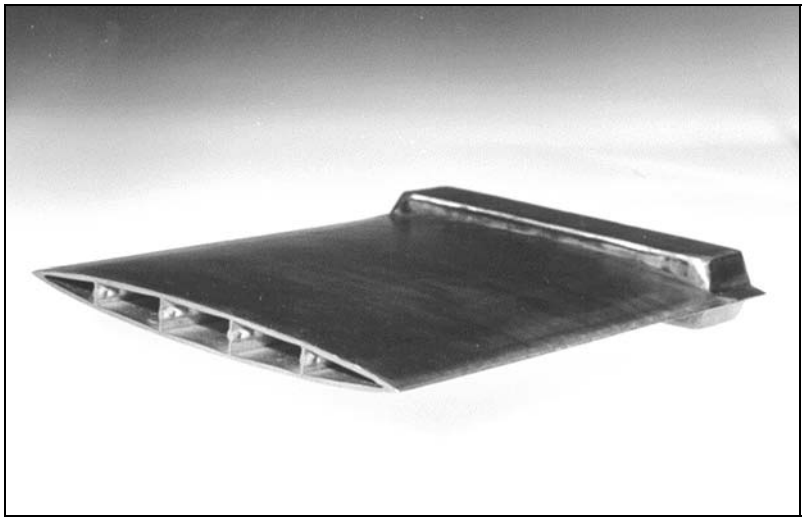

Fig. 4. Model of the hollow blade of a gas-turbine engine fabricated by the integrated technology of welding by pressure with superplastic molding from the VT6 alloy at the temperature that did not exceed $T = 800°C$.

hollow blade of a gas-turbine engine (Fig. 4) [64]. With the application of nanomaterials, this product is fabricated at technologically convenient reduced temperatures and has improved operational properties.

The above-indicated prospects for application of nanomaterial are based on the capability of the DNM method, in particular, of the HIF method, to provide the assortment of nanostructured semifinished items required for industrial applications. With the help of the HIF method, sheets of industrial dimensions (1500 × 500 × 2 mm) with the grain size $d = 500$ nm were produced in [31] by rolling at relatively low temperatures of bulk billets with dimensions of ∅150 × 200 mm. If necessary, the dimensions of semifinished items can be increased significantly, since in this respect, the method has no principal limitations.

CONCLUSIONS

A little more than 20 years have passed since the publication of works that first demonstrated the possibility of application of plastic deformation to produce metals with grain sizes of about 100 nm [15, 16]. During this time, a new direction in physical materiology connected with the deformation methods of nanostructuring was organized and rapidly developed. The aim of the present work has been to illustrate the origin of this direction and its prospects as well as to give a certain DNM classification based on the fundamental mechanisms of structurization under plastic deformation. These mechanisms define two radically different approaches to the DNM: severe plastic deformation at low temperatures and soft plastic deformation based on the dynamic recrystallization for material nanostructuring. A large number of new DNM schemes are technical implementations of these two approaches, and their efficiencies and application fields should be primarily analyzed from this viewpoint. The tendency in the development of investigations in this area gives us grounds to believe that with deeper understanding of laws of nanostructuring by the deformation methods, bulk nanomaterials will find wide application in various technologies.

This work was supported in part by the Russian Foundation for Basic Research (grant No. 06-08-00802).

REFERENCES

1. H. Gleiter, Progr. Mater. Sci., **33**, No. 4, 223–315 (1989).
2. A. I. Gusev and A. A. Rempel', Nanocrystalline Materials [in Russian], Fizmatlit, Moscow (2000).

3. N. I. Noskova and R. R. Mulyukov, Submicrocrystalline and Nanocrystalline Metals and Alloys [in Russian], Publishing House of the Ural Branch of the Russian Academy of Sciences, Ekaterinburg (2003).
4. R. Z. Valiev and I. V. Aleksandrov, Bulk Nanostructural Materials: Synthesis, Structure, and Properties [in Russian], Nauka, Moscow (2007).
5. A. A. Nazarov and R. R. Mulyukov, in: Engineering and Technology Handbook, S. Lyshevski, D. Brenner, J. Iafrate, and W. Goddard, eds., CRC Press, Boca Raton (2002), pp. 22–1–22–41.
6. R. R. Mulyukov, Ross. Nanotekhnol., **2**, Nos. 7–8, 38–53 (2007).
7. I. D. Morokhov, L. I. Trusov, and L. P. Chizhik, Ultradisperse Metal Media [in Russian], Atomizdat, Moscow (1977).
8. Y. Zhu and T. G. Langdon, J. Miner., Metals Mater. Soc., **56**, No. 10, 58–64 (2004).
9. R. Z. Valiev, Y. Estrin, X. Horita, *et al*., J. Miner., Metals Mater. Soc., **58**, 33–39 (2006).
10. N. A. Koneva and É. V. Kozlov, Russ. Phys. J., No. 2, 165 (1990).
11. V. I. Trefilov, Yu. V. Mil'man, and S. A. Firstov, Physical Principles of Strength of Refractory Metals [in Russian], Naukova Dumka, Kiev (1975).
12. V. V. Rybin, Severe Plastic Deformations and Fracture of Metals [in Russian], Metallurgiya, Moscow (1986).
13. O. A. Kaibyshev, Superplasticity of Industrial Alloys [in Russian], Metallurgiya, Moscow (1984).
14. Zh. P. Puar'e, The High-Temperature Plasticity of Crystalline Bodies [Russian translation], Metallurgiya, Moscow (1982).
15. N. A. Smirnova, V. I. Levit, V. I. Pilyugin, *et al*., Fiz. Met. Metalloved., **61**, 1170–1177 (1986).
16. N. A. Smirnova, V. I. Levit, V. I. Pilyugin, *et al*., Fiz. Met. Metalloved., **62**, 566–570 (1986).
17. A. V. Korznikov, S. R. Idrisova, O. Dimitrov, *et al*., Fiz. Met. Metalloved., **85**, No. 5, 91–95 (1998).
18. M. V. Degtyarov, T. I. Chashchukhina, L. M. Voronova, *et al*., Acta Mater., **55**, 6039–6050 (2007).
19. Y. H. Zhao, X. Z. Liao, Y. T. Zhu, *et al*., Mater. Sci. Eng., **A410–A411**, 188–193 (2005).
20. V. I. Kopylov and V. I. Chuvil'deev, in: Severe Plastic Deformation: toward Bulk Production of Nanostructured Materials, B. S. Altan, ed., Nova Science, New York (2006), pp. 37–58.
21. B. M. Segal, V. I. Reznikov, F. E. Drobyshevskii, and V. I. Kopylov, Izv. Akad. Nauk SSSR, Metally, No. 1, 115–123 (1981).
22. V. M. Segal, Mater. Sci. Eng., **A271**, 322–333 (1999).
23. N. A. Akhmadeev, R. Z. Valiev, V. I. Kopylov, and R. R. Mulyukov, Metally, No. 5, 96–101 (1992).
24. G. J. Raab, R. Z. Valiev, T. C. Lowe, and Y. T. Zhu, Mater. Sci. Eng., **A382**, 30–34 (2004).
25. D. A. Hughes, N. Hansen, and D. J. Bammann, Scripta Mater., **48**, 147–153 (2003).
26. Y. Iwahashi, Z. Horita, M. Nemoto, and T. G. Langdon, Acta Mater., **46**, No. 9, 3317–3331 (2008).
27. Y. T. Zhu and T. C. Lowe, Mater. Sci. Eng., **A291**, 46–53 (2000).
28. A. Gholinia, P. B. Prangnell, and M. V. Markushev, Acta Mater., **48**, 1115–1130 (2000).
29. J. H. Driver, Scripta Mater., **51**, 819–823 (2004).
30. G. Zhao, S. Xu, Y. Luan, *et al*., Mater. Sci. Eng., **A437**, 281–292 (2006).
31. R. O. Valiakhmetov, R. M. Galeev, and G. A. Salishchev, Fiz. Met. Metalloved., **72**, No. 10, 204–206 (1990).
32. R. M. Imayev and V. M. Imayev, Scripta Met. Mater., **25**, 2041–2046 (1991).
33. G. A. Salishchev, O. R. Valiakhmetov, and R. M. Galeev, J. Mater. Sci., **28**, 2898–2902 (1993).
34. R. M. Imayev, V. M. Imayev, and G. A. Salishchev, J. Mater. Sci., **27**, 4465–4471 (1992).
35. S. V. Zherebtsov, G. A. Salishchev, R. M. Galeyev, *et al*., Scripta Mater., **51**, 1147–1151 (2004).
36. R. Z. Valiev, A. V. Korznikov, and R. R. Mulyukov, Mater. Sci. Eng., **A168**, 141–148 (1993).
37. R. Z. Valiev, A. V. Korznikov, and R. R. Mulyukov, Fiz. Met. Metalloved., **76**, No. 4, 70–86 (1992).
38. R. Z. Valiev and R. S. Musalimov, Fiz. Met. Metalloved., **78**, No. 6, 114–119 (1994).
39. R. Z. Valiev, R. R. Mulyukov, V. V. Ovchinnikov, *et al*., Metallofizika, **12**, No. 5, 124–126 (1990).
40. L. R. Zubairov, E. A. Litvinov, R. R. Mulyukov, *et al*., Dokl. Ross. Akad. Nauk, **372**, No. 3, 319–321 (2000).
41. R. R. Mulyukov, E. A. Litvinov, L. R. Zubairov, *et al*., Physica, **B324**, Nos. 1–4, 329–335 (2002).
42. E. A. Litvinov, R. R. Mulyukov, L. R. Zubairov, *et al*., Zh. Tekh. Fiz., **74**, No. 6, 96–101 (2004).
43. A. A. Nazarov, A. E. Romanov, and R. Z. Valiev, Scripta Mater., **34**, No. 5, 729–734 (1996).
44. A. A. Nazarov, Scripta Mater., **37**, No. 8, 1155–1161 (1997).

45. G. A. Salishchev, R. M. Galeev, and S. R. Malysheva, Metalloved. Termich. Obrab. Met., No. 2, 19–26 (2006).
46. G. A. Salishchev, O. R. Valiakhmetov, R. M. Galeev, and S. R. Malysheva, Metally, No. 4, 86–91 (1996).
47. G. A. Salishchev, R. M. Galeev, S. V. Zherebtsov, *et al*., Metally, No. 6, 84–87 (1999).
48. Sh. Kh. Mukhtarov, V. A. Valitov, and N. R. Dudova, Fizich. Mezomekh., **7**, No. 2, 38–41 (2004).
49. R. M. Imayev, N. K. Gabdullin, G. A. Salishchev, *et al*., Acta Mater., **47**, 1809–1821 (1999).
50. R. Würschum, A. Kubler, S. Gruss, *et al*., Ann. Chim., **21**, 471–482 (1996).
51. A. A. Nazarov, Phil. Mag. Lett., **80**, No. 4, 221–228 (2000).
52. A. A. Nazarov and R. T. Murzaev, TMS Lett., **3**, No. 2, 29–30.
53. N. A. Akhmadeev, R. Z. Valiev, N. P. Kobelev, *et al*., Fiz. Tverd. Tela, **34**, No. 10, 3155–3160 (1992).
54. R. R. Mulyukov and A. I. Pshenichnyuk, J. Alloys Comp., **355**, 26–30 (2003).
55. R. Z. Valiev, R. R. Mulyukov, Kh. Ya. Mulyukov, *et al*., Pis'ma Zh. Tekh. Fiz., **15**, No. 1, 78–81 (1989).
56. Kh. Ya. Mulyukov, G. F. Korznikova, and S. A. Nikitin, Fiz. Tverd. Tela, **37**, No. 8, 2481–2486 (1995).
57. Kh. Ya. Mulyukov, G. F. Korznikova, R. Z. Abdulov, and R. Z. Valiev, J. Magn. Magn. Mater., **89**, 207–213 (1990).
58. V. V. Stolyarov, A. G. Popov, D. V. Gunderov, *et al*., Fiz. Met. Metalloved., **83**, No. 2, 100–108 (1997).
59. G. F. Korznikova, Deform. Razr. Mater., No. 2, 25–29 (2006).
60. G. F. Korznikova, Metalloved. Termich. Obrab. Mater., No. 2, 33–37 (2006).
61. R. K. Islamgaliev, N. A. Akhmadeev, R. R. Mulyukov, and R. Z. Valiev, Metallofizika, No. 2, 317–320 (1990).
62. R. R. Mulyukov and Yu. M. Yumaguzin, Dokl. Ross. Akad. Nauk, **399**, No. 6, 730–732 (2004).
63. A. A. Kruglov, R. Ya. Lutfullin, M. Kh. Mukhametrakhimov, *et al*., Perspekt. Mater., No. 6, 79–85 (2005).
64. R. Ya. Lutfullin, O. A. Kaibyshev, O. R. Valiakhmetov, *et al*., Perspekt. Mater., No. 4, 21–25 (2003).